An Acad Bras Cienc (2022) 94(Suppl. 1): e20210797 DOI 10.1590/0001-3765202220210797
Anais da Academia Brasileira de Ciências | *Annals of the Brazilian Academy of Sciences*
Printed ISSN 0001-3765 I Online ISSN 1678-2690
www.scielo.br/aabc | www.fb.com/aabcjournal

GEOSCIENCES

Using wavelet decomposition method to retrieve the solar and the global air temperature signals from Greenland, Andes and East Antarctica $\delta^{18}O$ ice core records

HEITOR EVANGELISTA, MARIZA P. DE SOUZA ECHER & EZEQUIEL ECHER

Abstract: The surface global air temperature (SGAT) and the solar activity presented near similar trends until approximately the 1980's decade, when they start to diverge significantly. This divergence in both time series is attributed to the impact of addition players acting in the climate system as the greenhouse gas emissions and a more active ENSO (El Niño Southern Oscillation). For the period before this "turning point" we have made an exploratory investigation on the imprint of both SGAT and the solar activity (represented by the Sunspot Number – SSN) at $\delta^{18}O$ isotopic ratios retrieved from ice cores, a proxy commonly used to describe past climate changes. In this work $\delta^{18}O$ isotopic ratios, dated from 1861 to 1997, from three distinct global sites: (1) the Greenland Ice Sheet Project 2 (GISP2); (2) Quelccaya ice cap/Andes (Peru); and (1) Dronning Maud Land (DML)/East Antarctica were investigated. The wavelet decomposition method and regressions applied to these databases successfully allowed the isotopic reconstructions from both SGAT and SSN. We found that the reconstructions differ significantly depending on the geographical site.

Key words: climate change, ice cores, oxygen isotopes, solar activity, solar-climate relationship.

INTRODUCTION

The solar impact in the Earth's climate is manifested in different ways and in different time scales. Along the last eight glacial cycles during the Pleistocene, the European Project for Ice Coring in Antarctica (EPICA) ice core, revealed an apparent dependence of climate parameters to the incoming solar radiation due to Earth's orbital parameters (EPICA community members 2004). On the time scale from decades to centuries, when the orbital forcing contributes less, the physical processes that take place in the sun's photosphere (represented by the solar irradiance, solar length, Sunspot Number – SSN – and related parameterizations) contributed to explain the Earth's climate changes in the North Hemisphere, especially when associated with volcanism (Friis-Christensen & Lassen 1991, Lassen & Friis-Christensen 1995). The coincidence of Maunder's prolonged solar minimum and a global active volcanism with the coldest excursion of the Little Ice Age has long been noted by many researchers who have looked at the possible connections between the Sun and terrestrial climate (Eddy 1976 and references therein). During the Little Ice Ace it is estimated that the temperature in some places

was 1.0 to 1.5^{0}C colder than present (Crowley & North 1991, Bradley & Jones 1993, Mann et al. 2008). Nevertheless, it was clearly stated by the IPCC assessment reports editions the fact that the present satellite database, with regards to the solar irradiance monitoring, is still very short to consistently demonstrate the true impact of changes in solar activity over the Earth's climate (Souza-Echer et al. 2008, 2009, Rigozo et al. 2010, Myhre et al. 2013). Further there are also estimates of the solar impact on the Northern Hemisphere temperature based on proxy data (e.g. Schurer et al. 2014).

Stable isotopes of oxygen, $\delta^{18}O$, measured in ice cores, have been widely used as a regional temperature proxy. Within the water cycle, physical processes such as evaporation, condensation and thermal diffusion result in the isotopic fractioning of the oxygen and hydrogen that constitute the water molecule. Besides that, fractionation is also present along the pathway of the moist air parcels in the atmosphere, while over the oceans, mainland or when they ascend (Dansgaard 1964, Thompson et al. 2000). In the case of transport from the subtropics to the high latitudes, progressive removal of heavier oxygen isotope occurs. Additionally, the sea ice melting may change the coastal isotope signature directly by releasing latent heat. Taking into account these processes, from evaporation in the free atmosphere up to the final snow deposition in remote sites (polar regions or high mountains), a substantial change in the water vapor isotopic composition is expected to occur. In addition to that, the radiative input from the Sun is globally redistributed by the large scale transport of water vapor as latent heat. Considering that the solar radiation is directly or indirectly involved in all the above steps of the isotopic fractionation and a driver component of the Surface Global Air Temperature (SGAT) variability, we would expect that both signals would be present at $\delta^{18}O$ time series obtained from the global cryosphere. In this work we have employed $\delta^{18}O$ time series since the year 1860 from Antarctica, the Central Andes and Greenland aiming to investigate whether an imprint of the solar activity does exist in this isotope and SGAT time series, despite the fact that other parameters affect their variability.

In the search for the SSN and SGAT signals, we made use of a wavelet multi-resolution analysis (MRA). We performed the MRA on $\delta^{18}O$, SSN and SGAT time series by using Meyer wavelet. This is an orthonormal wavelet transform, which is composed of a mother wavelet and a scaling function. The Meyer wavelet allows the decomposition of an original signal into simpler oscillatory signals, such that their sum is robust in reconstructing the original signal (Percival & Walden 2000). It works like a band-pass filter in n different frequencies, each one limited by powers of 2 (i.e., 2^{n}, where n is related to the time series steps). By retrieving the above signals, we are able to infer the explained variance of the $\delta^{18}O$ time series with respect to the parameters SSN and SGAT. The content of this work is presented as follows. In Section 2, we present the datasets and the methods for data processing and analysis. In Section 3, we show the results, In Section 4 discussions and in the last Section conclusions.

MATERIALS AND METHODS

Isotopic databases

In this work, we have employed 3 ice core databases geographically distributed around the globe spanning approximately the same time interval. They were obtained from Dronning Maud Land (DML)/East Antarctica (75^{0}23'S,0^{0}70'E; 2882 m above sea level; Graf et al. 2002); Quelccaya ice cap/Andes/Peru (13^{0}56'S,070^{0}50'W; 5670 m above sea level; Thompson et al. 2000); and the Greenland

Ice Sheet Project 2 (GISP2) (71^{o}N,322^{o}E; 3200 m above sea level; White et al. 1997). The ice core from DML spans the time interval 1861-1997, while GISP2 and Peru ice core samples cover the period from 1861 to 1984. This corresponds approximately to the industrial epoch and the sprouting of meteorological stations worldwide. The $\delta^{18}O$ time series are available at PANGAEA website - Publishing Network for Geoscientific & Environmental Data (www.pangaea.de). The SSN is the longest solar data available which gives an indication of the general state of solar activity (Eddy 1976, Rigozo et al. 2001, 2008, Echer et al. 2004, 2005). The SSN database was obtained from the National Geophysical Data Center/USA web site; the SGAT database refers to the longest-running near-surface instrumental record of quasi-global coverage, that began in 1850. The global 2ς uncertainty in SGAT is estimated to be 0.16° C for the period 1861 to 2000 (Folland et al. 2001). These dataset time series are shown in Figure 1.

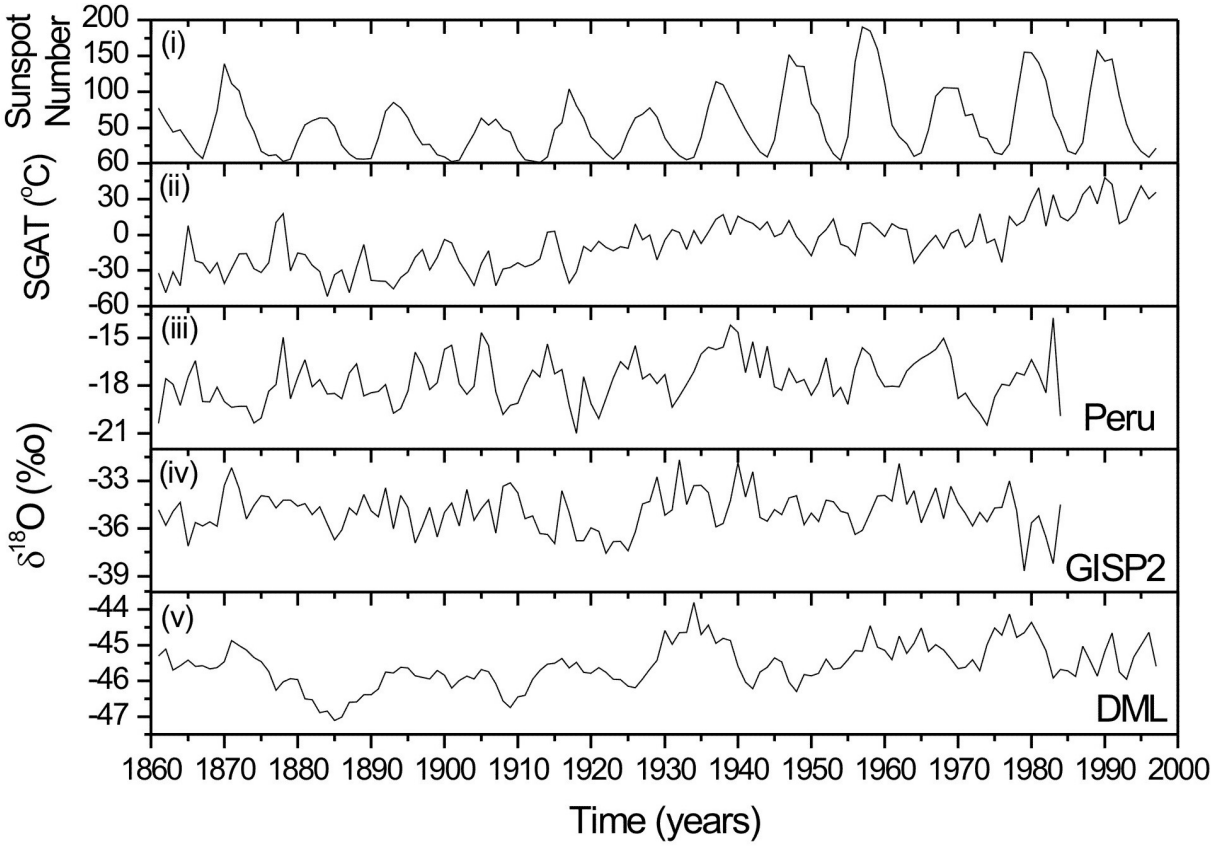

Figure 1. Time series for solar activity, air temperature and ice core oxygen isotopic data used in this work : (i) SSN, (ii) SGAT, (iii) $\delta^{18}O$ – Peru, (iv) $\delta^{18}O$ – GISP2 and (v) $\delta^{18}O$ - DML.

Mathematical methods

The investigation of the solar and climate imprints in the $\delta^{18}O$ time series was based in a data set of analysis: (1) the Morlet wavelet analysis and the cross-wavelet power analysis between $\delta^{18}O$ and SSN and $\delta^{18}O$ and SGAT time series, (Torrence & Compo 1998, Percival & Walden 2000); (2) the multi-resolution wavelet signal decomposition analysis (Percival & Walden 2000); (3) correlation and

regression analysis; (4) the Student-t hypothesis test to provide statistical significance to the r-Pearson values of the correlation analysis.

The wavelet transform is a spectral analysis technique well suited to analyze non-stationary time series. When one applies the wavelet transform to a time series, it decomposes it in translated and scaled (dilated or compressed) versions of the mother wavelet, each one multiplied by an appropriate coefficient. By varying the wavelet scale and translating along the localized time index, one can obtain a dynamic spectrum, or wavelet map, showing both the amplitude of any feature versus the scale and how this amplitude varies with time. In this work we used the complex Morlet wavelet which is a plane wave modulated by a Gaussian function. It is a powerful tool for non stationary signal analysis because it permits to identify the main periodicities in a time series and their evolution (Torrence & Compo 1998, Percival & Walden 2000).

The cross-wavelet analysis was used to identify common cyclicities between the parameters, their statistical significance and their strength (wavelet spectral power) variation over time. This is computed by taking the convoluted product between the wavelet transform of one-time series and the complex conjugated of the wavelet transform of the other time series (Torrence & Compo 1998, Grinsted et al. 2004).

In MRA, the signal (S) is decomposed in approximations (A) and in details (D). The details contain the high-frequency part of the signal and they are inserted in a period range limited by 2^n and 2^{n+1}, while the approximations contain most of the characteristic frequencies of the signal. In the first step of the decomposition, the signal has a low band pass filtered component, the A1 level, and a high band pass filtered component, the D1 level, such as S=A1+D1. In a next step, A1 is then split itself in 2 frequency levels, resulting in a A2+D2 signal, and one has the D2 level as the next bandpass high frequency level, A1=A2+D2, thus S=A2+D2+D1, and so on (Kumar & Foufoula-Georgiou 1997, Souza-Echer et al. 2009, 2012). In our analysis, the wavelet decomposition was performed until the D7 level. Therefore, the Meyer wavelet transform was applied here to the data with the objective to decompose them into orthonormal frequency levels. The decomposition levels D_j (j=1...,7) were obtained for δ^{18}O, SSN and SGAT. The frequency bands corresponding to each decomposition level used in this paper are D_1 (2-4 yr), D_2 (4-8 yr), D_3 (8-16 yr), D_4 (16-32 yr), D_5 (32-64 yr), D_6 (64-128 yr) and D_7 (128-256 yr), respectively.

Once we obtained the decomposed oscillatory signals (filtered data) from δ^{18}O time series of GISP2, Peru and DML, we correlated them with the corresponding decomposed levels of SSN and SGAT and then defined a multiple regression as given by equations (1) and (2):

$$\delta^{18}O_{\mathrm{SSN}}(t) = \sum_{i=1}^{n} [\alpha_i + \beta_i \mathrm{SSN}(t)_i] \tag{1}$$

and

$$\delta^{18}O_{\mathrm{SGAT}}(t) = \sum_{j=1}^{m} [\alpha_j + \beta_j \mathrm{SGAT}(t)_j] \tag{2}$$

Where n and m are the number of decomposed levels, and $\alpha_{i,j}$ and $\beta_{i,j}$ are respectively the linear and angular coefficients of the regression linear fit at the decomposed level D_j. For the determination of coefficients in (1) and (2), only statistically significant correlations were employed (n,m ≤ 7). To investigate which database (SSN or SGAT) allowed a better reconstruction of the original δ^{18}O time

series, we tested the significance of the difference between two dependent correlations. Therefore, r_{12} refers to the r-Pearson between $\delta^{18}O_{data}$ (original data) and $\delta^{18}O_{ssn}$ (reconstructed by SSN) and r_{13} refers to the r-Pearson between $\delta^{18}O_{data}$ (original data) and $\delta^{18}O_{SGAT}$ (reconstructed by SGAT). These r_{12} and r_{13} coefficients are used to evaluate the reconstructions.

The Student-t model used in this case is the Williams' modified (WM test) formula cited by Hendrickson et al. (1970) and given by equation 3:

$$t = (r_{12} - r_{13}) \frac{\sqrt{\{(n-1)(1+r_{23})\}}}{\sqrt{\left\{2\frac{(n-1)}{(n-3)}|R| + \frac{1}{4}(r_{12}-r_{13})^2(1-r_{23})^3\right\}}} \quad (3)$$

where $|R| = 1 - r_{12}^2 - r_{13}^2 - r_{23}^2 + 2r_{12}r_{13}r_{23}$ and r_{23} refers to r-Pearson coefficient between $\delta^{18}O$ reconstructed functions by SSN and SGAT. For the above model, the degree of freedom is computed as n-3. Comparisons of correlations were made by a two-tailed Student-*t* test at 95% confidence interval.

RESULTS

Cross wavelet analysis

Figure 2 shows the cross-wavelet spectra for $\delta^{18}O$, SSN and SGAT. From top to bottom are plotted the cross-wavelet dynamic spectra for DML/Antarctica, Quelccaya/Peru and GISP2/Greenland. It can be seen for $\delta^{18}O$ and SSN, Figure 2 (A_1, B_1 and C_1), a strong and persistent 8-16 yr cyclicity band existing at the 3 study sites, with higher cross-wavelet power and statistical significance between ~1920 and 1994. It can be noted that the time interval corresponding to the above cyclicity lies inside the domain of the cone of influence (COI) (white curved line crossing the wavelet spectrum). The statistical significance is given by the contour lines in the cross-wavelet dynamical spectra, which are shown here at 95% confidence level. This cyclicity can be attributed to the influence of the well known Schwabe cycle (~11 yr), which is the main harmonic of the sunspot number and total solar irradiance (TSI) variability. The observation of this quasi-periodic signal simultaneously in East Antarctica, Andes and Greenland may represent the global impact of the solar variability over the climate, transport of moisture, cloud formation among other variables that are ultimately reflected in the $\delta^{18}O$ variability. By contrast, the cross-wavelet analysis between $\delta^{18}O$ and SGAT revealed two intense multi-decadal signals: one occurs from ~1865 to 1901, at the ~16-32 yr band, closely aligned to the 22 yr Hale solar cycle, and the other from ~1920 to 1990, at the ~33-67 yr band. The 22-yr cyclicity, seen in the 16-32 yr band, is naturally produced by the 22-yr solar magnetic polarity cycle (Mursula et al. 2001). In the polar regions of East Antarctica and Greenland, only a sparse 22-yr imprint is recognized from $\delta^{18}O$ x SSN cross-wavelet, Figure 2 (A_1 and C_1). The persistence of Hale cyclicity in great part of the time series reflects the fact that its amplitude has been maintained relatively stable for centuries although with amplitude around 10% of the last decades sunspot activity level (Mursula et al. 2001, Hathaway 2015).

The cross-wavelet results shown in Figure 2 (for all the 3 sites) indicate that the 11-yr solar cycle imprint over $\delta^{18}O$ time series is only of statistical significance after ~1920-1930. It is seen from Figure 1(i) that SSN increases towards the end of 20^{th} century, especially after the strong rise in SSN noted in the 1930s. In our database, the mean SSN before 1930 is 88.8 while the mean SSN after 1930 is 145.9. This represents a significant change in solar activity and suggests that if the solar variability had any

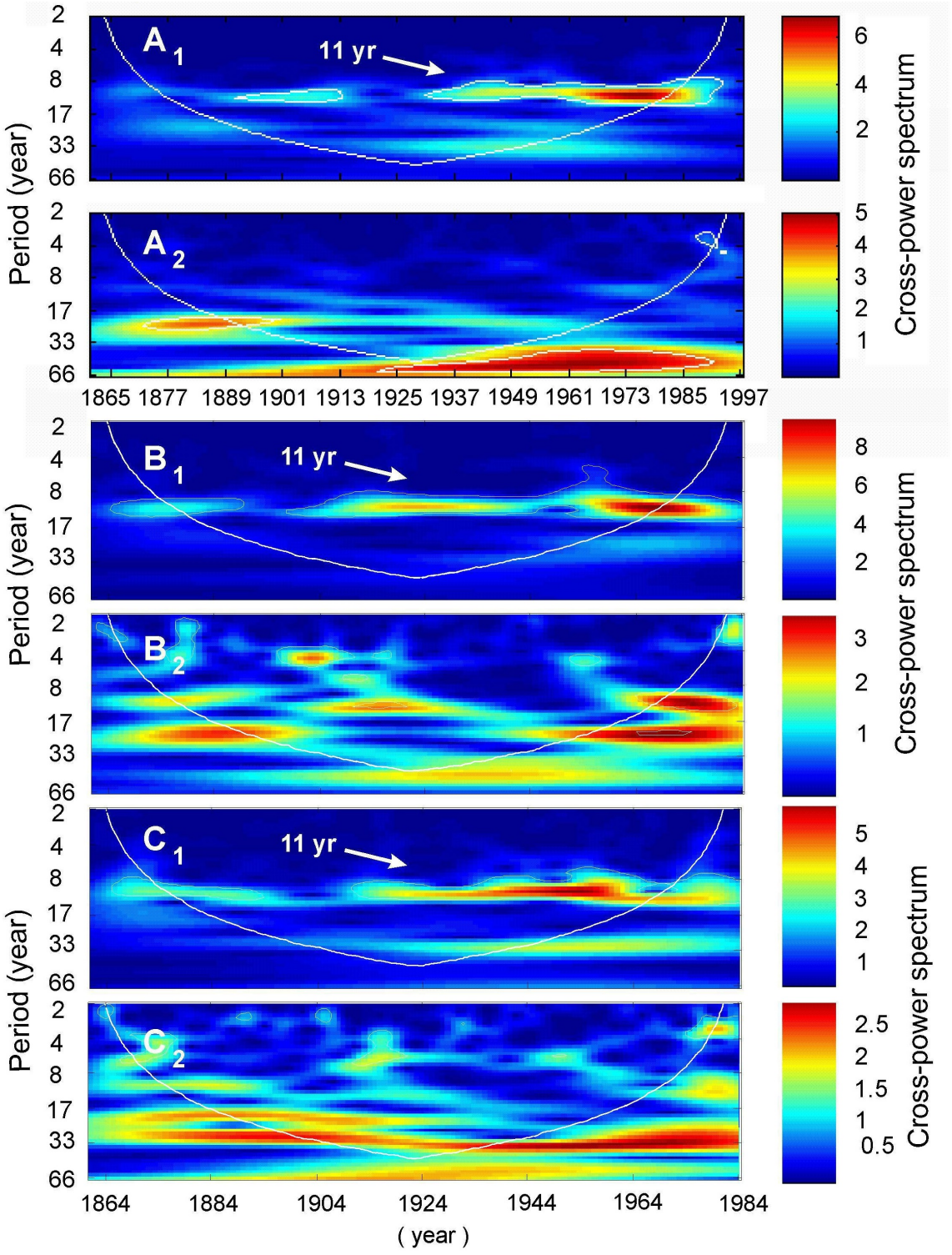

Figure 2. Wavelet cross-power spectra between $\delta^{18}O$ and SSN (A_1) and $\delta^{18}O$ and SGAT (A_2) for DML/Antarctica; $\delta^{18}O$ and SSN (B_1) and $\delta^{18}O$ and SGAT (B_2) for Quelccaya/Peru; and $\delta^{18}O$ and SSN (C_1) and $\delta^{18}O$ and SGAT (C_2) for GISP2/Greenland. The 11 yr period is indicated by a white arrow. Contour lines within the wavelet spectra indicate intervals significant at 95% confidence level. The quase-paraboloidal curve seen in all spectra is the cone of influence (COI) line.

influence on oxygen stable isotopes fractionation, this influence is probably constrained to a lower limit in solar variability intensity. A comparison of Figure 1(i) and Figure 2(A_1, B_1 and C_1), indicates that a detectable response in $\delta^{18}O$, between 1861 and 1997, of the 11 yr cyclicity may occur when the solar activity is more intense, SSN $\geq$ 100 (Hathaway 2015).

MRA decomposition of time series

Figure 3 show the MRA decomposition levels for SSN (on the left) and for SGAT (on the right) while Figure 4 shows MRA levels of $\delta^{18}O$ for DML (a) for the period 1861-1997. Andes/Peru (b) and GISP2 (c) for the period 1861-1984. Data were decomposed until the D7 level.

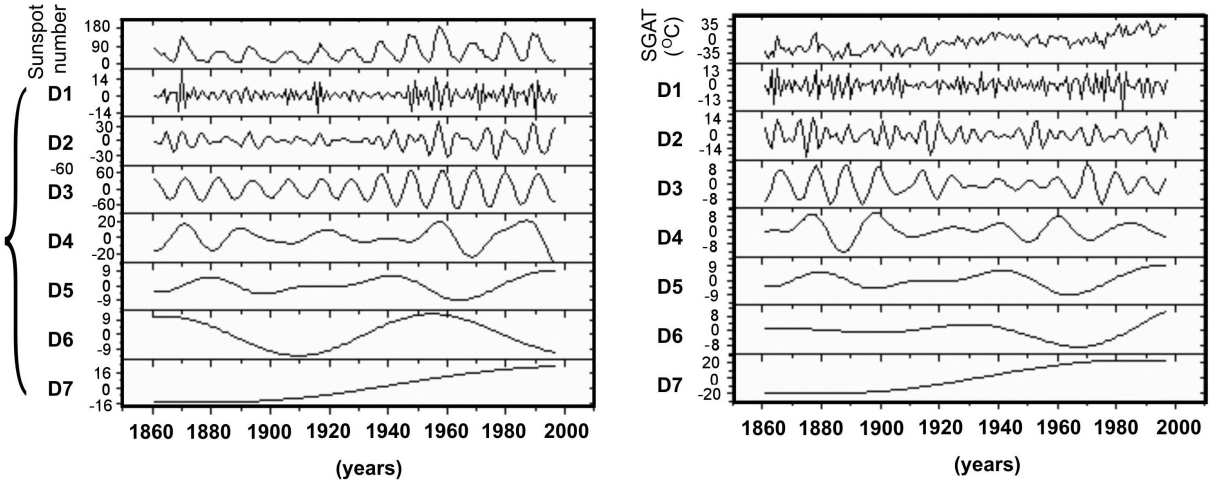

Figure 3. Sunspot number decomposition levels (left) and surface global air temperature decomposition levels (right) for the period 1861-1997.

Having obtained the decomposed levels, a linear regression was made at corresponding D_j levels between $\delta^{18}O$ and SSN and $\delta^{18}O$ and SGAT. Table I summarizes the r-Pearson correlation coefficients between oscillatory functions (or filtered frequency levels) obtained from the MRA decomposition method. Phase lags between oscillatory signals are also presented.

Taking into account the correlations among the original data of SGAT and $\delta^{18}O$, we found statistical significance at the study sites with the exception of GISP2 data. The correlation coefficients were the following: r=0.42 between SGAT and $\delta^{18}O_{Peru}$, r=0.40 between SGAT and $\delta^{18}O_{DML}$ and r=0.006 between SGAT and $\delta^{18}O_{GISP2}$. A basic difference existing among these sites that could be related to the $\delta^{18}O$ response is that both Quelccaya and DML sites are highly impacted by the direct and predominant action of marine air masses, which are associated with simpler regional hydrological cycles pathways. In the case of GISP2/Greenlad, ice cores show that annual $\delta^{18}O$ (and also its accumulation) is positively correlated to the North Atlantic Oscillation (NAO) (Sjolte et al. 2011, 2018). This means that this site become warmer with less sea ice during the NAO negative mode and colder with increased sea ice during the positive NAO mode, and therefore receives high influence of the North Atlantic sea surface temperature variability (Wanner et al. 2001, Faber et al. 2017).

From Figure 1, one can observe that $\delta^{18}O$ variability fluctuations in Andes/Peru and GISP2 are higher and of comparable magnitudes (s.d.=1.47 ‰ and 1.27 ‰, respectively) while DML preserves

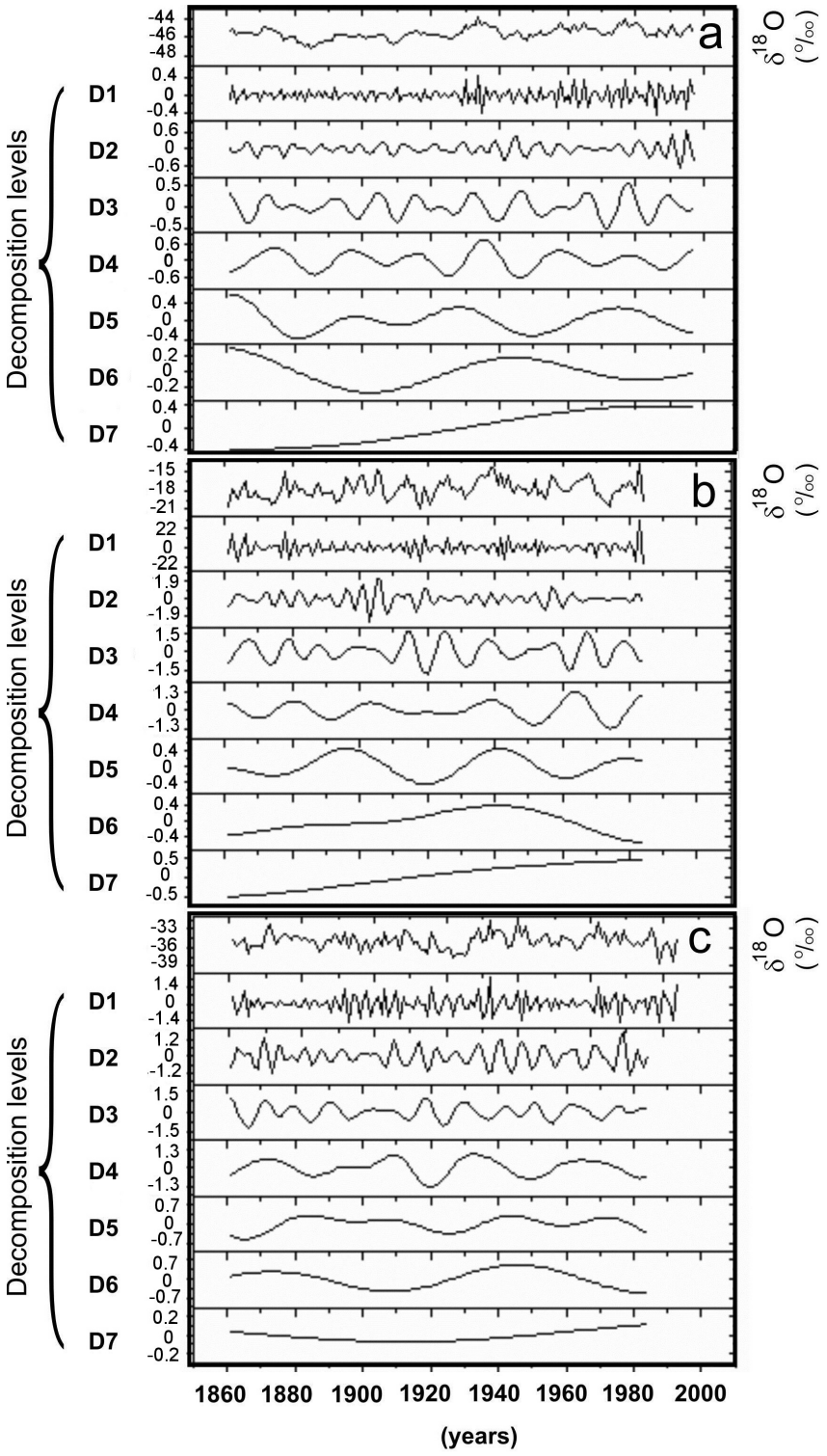

Figure 4. Decomposition levels of $\delta^{18}O$ for DML (a) for the period 1861-1997. Andes/Peru (b) and GISP2 (c) for the period 1861-1984.

Table I. Correlation coefficients obtained among decomposed levels of $\delta^{18}O$, SNN and SGAT. Values in bold are statistically significant at 95%.

Levels	r-Pearson coefficient of correlation (phase lag in years)					
	DML (Antarctica)		Quelccaya (Peru)		GISP2 (Greenland)	
	$\delta^{18}O$ x SNN	$\delta^{18}O$ x SGAT	$\delta^{18}O$ x SNN	$\delta^{18}O$ x SGAT	$\delta^{18}O$ x SNN	$\delta^{18}O$ x SGAT
D_1	-0.33 (+4)	-0.26 (+23)	-0.20 (6)	0.23 (0)	0.25 (-20)	-0.26 (2)
D_2	**-0.41** (-48)	-0.30 (+83)	-0.27 (38)	**-0.51** (2)	-0.35 (8)	0.34 (-6)
D_3	**0.56** (-2)	-0.36 (0)	**0.56** (9)	**0.50** (0)	-0.37(-23)	**-0.53** (-2)
D_4	**0.59** (-24)	**0.83** (-3)	**-0.56** (-5)	**0.75** (3)	**-0.58** (-35)	**0.62** (33)
D_5	**0.57** (+19)	**-0.65** (+1)	**0.93** (-10)	**-0.62** (-18)	**0.48** (-12)	**-0.61** (-15)
D_6	**0.81** (-9)	**0.79** (-52)	**-0.76** (26)	**0.70** (-7)	**0.79** (-2)	**0.82** (4)
D_7	**0.99** (-3)	**0.99** (-2)	**0.93** (0)	**0.98** (0)	**0.78** (7)	**0.73** (16)

a smoother signal (s.d.=0.61 ‰) reflecting its continental isolation. Also, the cross-wavelet spectrum, Figure 2, depicts a more complex structure of cycles with respect to $\delta^{18}O$ x SGAT for Andes and GISP2 in the decadal domain. For SSN and the oxygen stable isotopes, no significant correlation was observed while using the original data, we found r=0.10 between $\delta^{18}O_{Peru}$ and SSN, r=0.03 for $\delta^{18}O_{GISP2}$ and r=0.24 for $\delta^{18}O_{DML}$. Moreover, the linear correlation between SGAT and SSN is poor (r=0.22). We will demonstrate that in the case of employing the correlation among the decomposed levels of each time series we detect statistical significance in the main cyclicity modes.

In Table I, D_1 and D_2 levels represent the high frequency oscillation modes in the time series. These frequency bands are close to the dominant ENSO oscillation of ~2-6yr, which is associated with several impacts over the tropical region of both hemispheres and is clearly imprinted at Quelccaya ice cap (Kitzberger et al. 2001). The lower amplitude of this signal at DML, in East Antarctica, confirms previous works suggesting that the predominant impacts of ENSO in Antarctica are found at the Antarctic Western sector, at Amundsen/Bellingshausen Seas, since during ENSO, changes occur in the Hadley Cell configuration changing the relative positioning of the jet stream in the subtropics and consequently the downwards heat flux to Western Antarctica

In the D_3 level, which encloses the 11yr Schwabe solar cycle, positive and significant correlations were found between $\delta^{18}O$ x SSN for DML/Antarctica and Peru (both with the same r-Pearson, r=+0.56). The basic difference between them is the phase lag of the oscillatory signal, that is, -2 yr in of case of $\delta^{18}O$ x SSN for DML and +9 yr in the case of Andes. A phase lag of 2 years is of the same order of magnitude of the uncertainty in $\delta^{18}O$ chronology of ice cores spanning the time scale of 130 yr. Therefore, at the D3 level, $\delta^{18}O$ and SSN at DML site can be considered of comparable phases. This finding evidenced an imprint of the 11-yr solar cyclicity for the Antarctic ice core. The same can not be deduced for the Andes, despite the high r-Pearson correlation coefficient obtained. For GISP2, the r-Pearson value for $\delta^{18}O$ x SSN was far bellow the statistical significance.

Both GISP2 and Andes/Peru $\delta^{18}O$ data were correlated with SGAT in the D3 level. The D4 level encompasses the Hale solar cycle of ~22 yr. Both correlations of $\delta^{18}O$ x SSN and $\delta^{18}O$ x SGAT were

significant at the 3 sites. Nevertheless, DML is positively correlated while GISP2 and Andes/Peru are anti-correlated. At D5 level, an anti-correlation was found between $\delta^{18}O$ and SGAT and a weaker association between $\delta^{18}O$ and SSN. The D5, D6 and D7 levels encompass the Gleissberg (80 yr) and Suess (200 yr) solar cycles. The correlations in these levels are high for both $\delta^{18}O$ x SSN and $\delta^{18}O$ x SGAT at the 3 sites. Nevertheless these correlations should be interpreted with caution since high time-lag values do not support a direct causal relationship.

Using a robust reconstruction of solar variability proposed by Usoskin et al. (2007) for the Holocene (5000 - 1995 AD), Ma (2009), applying wavelet analysis, detected fluctuations of about 60–150 years in the solar activity attributed to the Gleissberg cycle. According to Ogurtsov et al. (2002), the Gleissberg cycle has a wide frequency band with a double structure, i.e., 50–80 year and 90–140 year cyclicities. With respect to the existing time lags in Table I, Sjolte et al. (2018) have analyzed the 11-year solar variability influence on the atmospheric circulation in the North Hemisphere by calculating the differences between reconstructed sea level pressure and surface air temperature. They found a strong response in the reconstructed sea level pressure and surface air temperature when lagging the solar forcing to 5 years for a region that enclosed the North Atlantic and Greenland. The relation between reconstructed sea level pressure and solar forcing is also noted for the centennial time scale when using ^{14}C-based solar reconstructions. The different time lags at different sites detected here led us to conclude that the water isotopic response to the solar cycles should be a complex issue and regionally constrained.

Reconstruction of $\delta^{18}O$ time series

Reconstruction of $\delta^{18}O$ time series was conducted by multi-regression functions (equations 1 and 2). Figure 5 depicts the reconstructed isotopic signals as a function of SSN and SGAT, superimposed over measured $\delta^{18}O$ for DML, GISP2 and Andes. We used all statistically significant r-Pearson coefficients obtained in the regressions (pointed in bold at Table I, that appear from D2 to D7), to achieve the reconstructed time series shown in Figure 5.

With respect to the significance of the reconstructed $\delta^{18}O$ from both SSN and SGAT, we obtained equivalent r-Pearson values and better reconstructions for the site DML, East Antarctica. For Andes/Peru, the isotopic reconstruction has a higher correlation with respect to SSN, while for GISP2, we observed that the reconstruction has a higher correlation with SGAT. The response of the temperature at global scale, due to the solar forcing, has been detected in previous studies such as the one conducted by Cubasch et al. (2004) who have performed simulations in which the solar signal could be isolated on longer timescales. These simulations allowed recognizing the Gleissberg cycle and the 11 year cyclicity of the Schwabe cycle at a global scale. Their results suggest a predominantly higher response of the Atlantic, Pacific and Indian Oceans at the tropical latitudinal band with decreasing correlations towards higher latitudes.

In our results we found that both GISP2 and Andes/Peru $\delta^{18}O$ time series were correlated with SGAT in the D_3 level (which encompasses the 11-year solar cycle signal). The D_4 level encompasses the Hale solar cycle of ~22 yr. Both correlations of $\delta^{18}O$ x SSN and $\delta^{18}O$ x SGAT were significant at the 3 sites. Nevertheless, DML is positively correlated while GISP2 and Andes/Peru data are anti-correlated to SSN. At D_5 level, an anti-correlation was found between $\delta^{18}O$ and SGAT, a weaker association between $\delta^{18}O$ and SSN was obtained, yielding a phase lag of +19 yr. The D_5, D_6 and D_7 levels encompass the Gleissberg

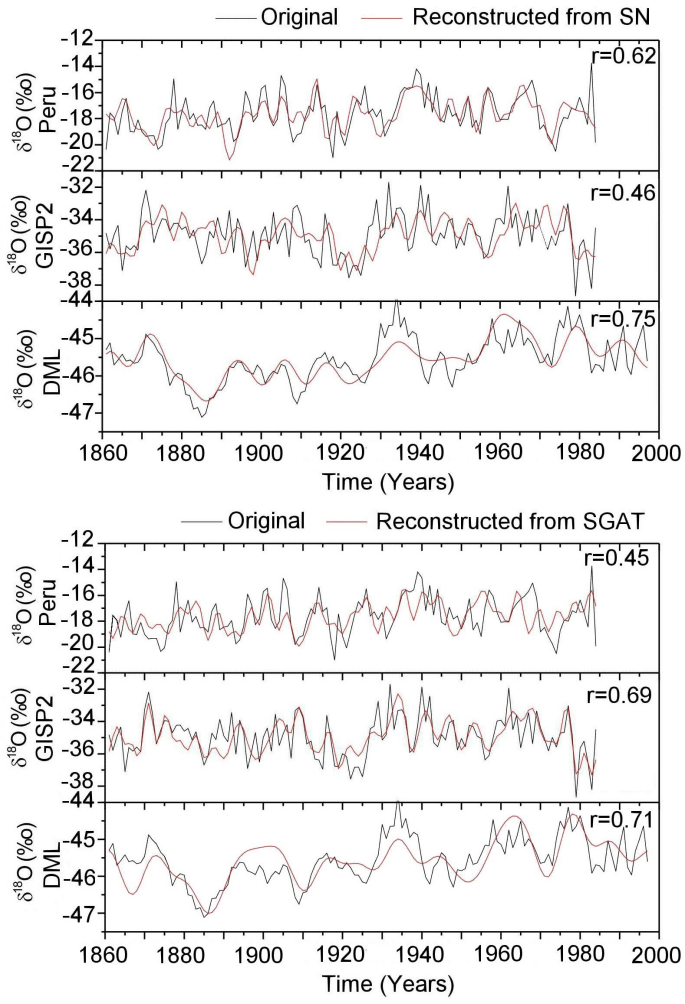

Figure 5. (top panel) Reconstructed and original $\delta^{18}O$ as a function of sunspot number for Peru, GISP2 and DML; (bottom panel) Reconstructed and original $\delta^{18}O$ as a function of surface global air temperature (SGAT) for Peru, GISP2 and DML.

(80 yr) and Suess (200 yr) solar cycles. The correlations in these levels are high for both $\delta^{18}O$ x SSN and $\delta^{18}O$ x SGAT at the 3 sites.

DISCUSSION

The sun-climate relationship is a very complex subject and the association between the atmospheric circulation and the solar variability is still a topic of controversy. Velasco & Mendoza (2008) have explored the relationship between the climatic indices such as the North Atlantic Oscillation (NAO), the Atlantic Multidecadal Oscillation (AMO), the Pacific Decadal Oscillation (PDO) and the Southern Oscillation Index (SOI), and obtained coherent variability among them and the solar activity, not only with respect to Schwabe cycle, but also to the Hale and Gleissberg cycles. Nevertheless, their work is not conclusive since they do not present a clear mechanism to explain their findings. It is far more acceptable nowadays that the solar influence over the global climate is indirect (Kodera &

Kuroda 2002). It has been argued that increased UV-radiation during the solar maximum (Wanner et al. 2008) may reinforce the solar component since it results in more ozone depletion and therefore in a cooler stratosphere. According to Turner et al. (2009) a cooler stratosphere does affects the atmospheric circulation at continental scale and consequently the transport of water vapor. The thermal stratification of the stratosphere and troposphere may also impact the Hadley Cell dynamics, the Indian Monsoon, the Northern Annular Mode (NAM) and probably the ENSO cycle (Wanner et al. 2008). Changes in these mechanisms may impact the global moisture transport and therefore the fractioning of oxygen isotopes. The phase lags obtained in the correlations showed in Table I are also found in terrestrial databases involving the hydrological cycle in the Northern Hemisphere. Perr (1995) reported significant correlations among precipitation, river stream flow, alluvial water level, glacier mass balance and the solar reconstructed irradiance in the USA since the 1950s. These hydro-meteorological and glaciological parameters were, in general, lagged 4 to 5 years with respect to the reconstructed solar irradiance model.

The imprint of solar irradiance on the (sub)tropical climate of South America, specially during the Little Ice Age (LIA), has been investigated by other terrestrial proxies as glacier advances and the flux of inorganic material to lake sediments in Venezuela (Polissar et al. 2006). These authors have presented evidences that during the past 1,500 yr, the precipitation regime at the site studied was highly dependent on the moisture transport. Despite the apparent small amplitude of total solar irradiance between the solar maximum and the solar minimum, 0.1% (Kopp & Lean 2011), the IPCC (since the 2007 edition, Fifth Assessment report - www.ipcc.ch) assumes that the Level of Scientific Understanding (LOSU) of solar radiation variability on Earth's climate is still considered low, because satellite irradiance measurements are available only from 1978 onwards. Although the changes in total irradiance is 0.1%, changes in UV band can reach as much as 10% between the solar minimum and maximum, strongly impacting the stratospheric photochemistry (Lean & Deland 2012).

Although our methods have confirmed that an imprint of the solar variability does exist on the $\delta^{18}O$ time series at both polar and tropical environments, it remains relatively uncertain how effectively the isotopic fractionation responds to the solar variability and how it changes along the hydrological cycle. The rise of new knowledge on changes of the solar spectral irradiance on the solar-Earth Climate link may have implications on cloud cover and consequently in the evaporation from oceans. It has been demonstrated, from controlled experiments, that evaporation from free water surfaces depend basically on the flux of solar radiation, molecular diffusivity, and wind speed as power-law dependence (Rohwer 1931). The most probable coupling mechanism between the incoming solar radiation and the global hydrological cycle still requires more detailed description of how changes in the lower stratosphere propagate to the lower levels and the resulting climatology is recorded by environmental proxies.

In our work, the correlations between reconstructed and measured $\delta^{18}O$ databases varied almost at the same range (from 0.46 to 0.75 using SSN and from 0.45 to 0.71 using SGAT). For GISP2 the reconstructed isotopic time series was better achieved by the SGAT than SSN, while for Peru/Andes it was the opposite. One explanation to this outcome is the fact that at most part of the North Hemisphere, air temperature has increased by a factor ranging from 2 to 4 ^{0}C while in Central and Southern Andes it was not higher than 0.2 ^{0}C, according to the GISS Surface Temperature Analysis Tool (http://data.giss.nasa.gov/gistemp). This difference is consistent with Cubasch et al. (2004) study

in which they isolated the solar signal on decadal time scales to obtain global spatially sensitivities to solar cycles. They found higher correlations over the tropical Atlantic and Indian Oceans, decreasing towards the higher latitudes. In this context, the better reconstruction we obtained at Andes with SSN may reflect that response.

CONCLUSIONS

This work is presently in an exploratory level in the use of MRA wavelet signal decomposition over $\delta^{18}O$ databases retrieved from ice-cores. Our results are promising and show a great potential of the method to be applied at longer databases and at different sites. The retrieved signals from Dronning Maud Land/East Antarctica, Andes/Peru and Greenland behaved as useful for extracting the main cyclic modes from climate databases despite the high noising component existing in the original data at the above sites. Correlations between the original and the reconstructed isotopic signals, obtained by the solar variability, showed statistical significant r-Pearson values ranging from 0.46 to 0.75. The same technique applied between $\delta^{18}O$ time series and the surface global air temperature (SGAT) resulted in reconstructions of r-Pearson values ranging from 0.45 to 0.71.

The $\delta^{18}O$ reconstructions for East Antarctica/DML were achieved for both SGAT and SSN at the same level of correlation (0.71 and 0.75, respectively). A possible explanation for this finding is that the SGAT and the solar activity behaved quite similarly from 1860 to ~1970 (Friis-Christensen & Lassen 1991). Additionally, the effects of rising air temperature due to greenhouse gases emissions in the remote Southern Hemisphere is less representative than at the North Hemisphere and the tropics, for the above period. In contrast, GISP2/Greenland oxygen isotopic database was better reconstructed by SGAT variability than by the solar activity. At the Andes, the solar signal was predominant.

Acknowledgments

The authors thank grants that supported this research: H.E, Silva - PROATEC grant by State University of Rio de Janeiro (UERJ) and Conselho Nacional de Desenvolvimento Científico e Tecnológico "INCT-Criosfera"/MCT/CNPq., M.P. Souza Echer - Coordenação de Aperfeiçoamento de Pessoal de Nível Superior (CAPES) (Grant: PNPD 88882.317520/2019-01 GES/INPE 33010013008P0); E. Echer - Fundação de Amparo à Pesquisa do Estado de São Paulo (FAPESP) (Grant:2018/21657-1) and Conselho Nacional de Desenvolvimento Científico e Tecnológico (CNPq) (Grant: 301883/2019-0). We would like to dedicate this paper to Nivaor Rodolfo Rigozo and Daniel Jean Roger Nordemann, who have done the work on signal and wavelet analysis during their life in space research. The authors declare to have no conflict of interest.

REFERENCES

BRADLEY RS & JONES PD. 1993. `Little Ice Age` summer temperature variations: Their nature and relevance to recent global warming trends. Holocene 3: 367-376.

CROWLEY TJ & NORTH GR. 1991. Paleoclimatology. Oxford University Press. New York, 360 p.

CUBASCH U, BURGER G, FAST I, SPANGEHL T & WAGNER S. 2005. The direct solar influence on climate: modeling the lower atmosphere. Mem S A It 76: 810-818.

DANSGAARD W. 1964. Stable isotopes in precipitation. Tellus 16(4): 436-468.

ECHER E, GONZALEZ WG, GONZALEZ ALC, PRESTES A, VIEIRA LEA, DAL LAGO A, GUARNIERI FL & SCHUCH NJ. 2004. Long-term correlation between solar and geomagnetic activity. J Atmos Sol Terr Phys 66: 1019-1025.

ECHER E, GONZALEZ WD, GUARNIERI FL, DAL LAGO A & VIEIRA LEA. 2005. Introduction to space weather. Adv Space Res 35: 855-865.

EDDY JA. 1976. The Maunder minimum. Science 192(4245): 1189-1202.

EPICA COMMUNITY MEMBERS. 2004. Eight glacial cycles from an Antarctic ice core. Nature 429: 623-629.

FABER AK, VINTHER BM, SJOLTE J & ANKER PEDERSEN R. 2017. How does sea ice influence $\delta^{18}O$ of Arctic precipitation? Atmos Chem Phys 17: 5865-5876.

FRIIS-CHRISTENSEN E & LASSEN K. 1991. Length of the solar cycle: an indicator of solar activity closely associated with climate. Science 254(5032): 698-700.

FOLLAND C ET AL. 2001. Global Temperature Change and Its Uncertainties Since 1861. Geophys Res Lett 28: 2621-2624. DOI: 10.1029/2001GL012877.

GRAF W, OERTER H, REINWARTH O, STICHLER W, WILHELMS F, MILLER H & MULVANEY R. 2002. Stable-isotope records from Dronning Maud Land, Antarctica. Ann Glaciol 35: 195-201.

GRINSTED A, MOORE JC & JEVREJEVA S. 2004. Application of the cross wavelet transform and wavelet coherence to geophysical time series. Nonlin Process Geophys 1: 561-566. (EGU).

HATHAWAY DH. 2015. The Solar Cycle. Living Rev Sol Phys 12: n. 4

HENDRICKSON GF, STANLEY JC & HILLS JR. 1970. Olkin's new formula for significance of r13 vs r23 compared with Hotelling's method. Am Educ Res J 7(2): 189-195.

KITZBERGER T, SWETNAM TW & EBLEN TT. 2001. Inter-hemispheric synchrony of forest fires and the El Niño-Southern Oscillation. Glob Ecol Biogeogr 10: 315-326.

KODERA K & KURODA Y. 2002. Dynamical response to the solar cycle. J Geophys Res D(24): Atmos 107: 4749. doi:10.1029/2002JD002224.

KOPP G & LEAN JL. 2011. A new lower value of total solar irradiance: Evidence and climate significance. Geophys Res Lett 38: L01706. doi:10.1029/2010GL045777.

KUMAR P & FOUFOULA-GEORGIOU E. 1997. Wavelet analysis for geophysical applications. Rev Geophys 35: 385.

LASSEN K & FRIIS-CHRISTENSEN E. 1995. Variability of the solar cycle length during the past five centuries and the apparent association with terrestrial climate. J Atmos Sol Terr Phys 57: 835-845.

LEAN JL & DELAND MT. 2012. How Does the Sun's Spectrum Vary? J Clim 25: 2555- 2560. doi: 10.1175/JCLI-D-11-00571.1.

MA LH. 2009. Gleissberg cycle of solar activity over the last 7000 years. New Astron 14: 1-3.

MANN ME, ZHANG Z, HUGHES MK, BRADLEY RS, MILLER KS, RUTHERFORD S & NI F. 2008. Proxy-based reconstructions of hemispheric and global surface temperature variations over the past two millennia. Proc Natl Acad Sci U S A 105(36): 13252-13257.

MURSULA K, USOSKI IG & KOVALTSOV GA. 2001. Persistent 22-year cycle in sunspot activity: evidence for a relic solar magnetic field. Sol Phys 198: 51-56.

MYHRE GD ET AL. 2013. Anthropogenic and Natural Radiative Forcing. In: Climate Change: The Physical Science Basis. Contribution of Working Group I to the Fifth Assessment Report of the Intergovernmental Panel on Climate Change [STOCKER TF et al. (Eds)]. Cambridge University Press, Cambridge, United Kingdom and New York, NY, USA, p. 659-740.

OGURTSOV MG, NAGOVITSYN YA, KOCHAROV GE & JUNGNER H. 2002. Long Period Cycles of the Sun's Activity Recorded in Direct Solar Data and Proxies. Sol Phys 211(1/2): 371-394. doi:10.1023/a:1022411209257.

PERCIVAL D & WALDEN A. 2000. Wavelet Methods for Time Series Analysis (Cambridge Series in Statistical and Probabilistic Mathematics). Cambridge: Cambridge University Press. doi:10.1017/CBO9780511841040.

PERR CA. 1995. Association between solar-irradiance variations and hydroclimatology of selected regions of the USA. In: Proceedings of the 6th International Meeting on Statistical Climatology, 19-23 June, Galway, Ireland, p. 239-242.

POLISSAR PJ, ABBOT MB, WOLFE AP, BEZADA M, RULLV & BRADLEY RS. 2006. Solar modulation of Little Ice Age climate in the tropical Andes. Proc Natl Acad Sci U S A. 103(24): 8937-8942.

RIGOZO NR, ECHER E, VIEIRA LEA & NORDEMANN DJR. 2001. Reconstruction of Wolf sunspot number on the basis of spectral characteristics and estimates of associated radio flux and solar wind parameters for the last millennium. Sol Phys 203: 179-191.

RIGOZO NR, EVANGELISTA H, NORDEMANN DJR, ECHER E, SOUZA ECHER MP & PRESTES A. 2008. The Medieval and Modern Maximum Solar Activity Imprints in Tree-ring data from Chile and Stable Isotope Records from Antarctica and Peru. J Atm Sol Terr Phys 70(7): 1012-1024.

RIGOZO NR, NORDEMANN DJR, ECHER E, ECHER MPS & EVANGELISTA H. 2010. Prediction of Solar Minimum and Maximum epochs on the basis of Spectral Characteristics for the next Millennium. Planet Space Sci 58: 1971-1976.

ROHWER C. 1931. Evaporation from free water surfaces. USDA Tech Bull 271, p. 96.

SCHURER AP ET AL. 2014. Small influence of solar variability on climate over the past millennium. Nat Geosci 7: 104.

SJOLTE J ET AL. 2011. Modeling the water isotopes in Greenland precipitation 1959-2001 with the meso-scale model REMO-iso. J Geophys Res D: Atmos 116: 18105-18126.

SJOLTE J ET AL. 2018. Solar and volcanic forcing of North Atlantic climate inferred from a process-based reconstruction. Clim Past 14: 1179-1194.

SOUZA-ECHER MP, ECHER E, NORDEMANN DJR & RIGOZO NR. 2009. Multi-resolution analysis of global surface air temperature and solar activity relationship. J Atmos Sol Terr Phys 71: 41-44.

SOUZA-ECHER MP, ECHER E, NORDERMANN DJR, RIGOZO NR & PRESTES A. 2008. Wavelet analysis of a centennial (1895-1994) southern Brazil rainfall series (Pelotas, $31^{o}46^{'}19^{"}$S $52^{o}20^{'}33^{"}$ W). Climatic Change 87: 489-497.

SOUZA-ECHER MP, ECHER E, RIGOZO NR, BRUM CGM, NORDEMANN DJR & GONZALEZ W. 2012. On the relationship between global, hemispheric and latitudinal averaged air surface temperature (GISS time series) and solar activity. J Atmos Sol Terr Phys 74: 87-93.

THOMPSON LG, MOSLEY-THOMPSON E & HENDERSON KA. 2000. Ice-core palaeoclimate records in tropical South America since the Last Glacial Maximum. J Quat Sci 15(4): 377-394.

TORRENCE C & COMPO GP. 1998. A Practical Guide to Wavelet Analysis. Bull Am Meteorol Soc 79: 61-78.

TURNER J, COMISO JC, MARSHALL GJ, LACHLAN-COPE TA, BRACEGIRDLE T, MAKSYM T, MEREDITH MP, WANG ZM & ORR A. 2009. Non-annular atmospheric circulation change induced by stratospheric ozone depletion and its role in the recent increase of Antarctic sea ice extent. Geophys Res Lett 36: L08502.

USOSKIN I G, SOLANKI SK & KOVALTSOV GA. 2007. Grand minima and maxima of solar activity: new observational constraints. Astron Astrophys 471: 301-309.

VELASCO VM & MENDONZA B. 2008. Assessing the relationship between solar activity and some large scale climatic phenomena. Adv Space Res 42: 866-878.

WANNER H, BRÖNNIMANN S, CASTY C, GYALISTRAS D, LUTERBACHER J, SCHMUTZ C, STEPHENSON DB & XOPLAKI E. 2001. North Atlantic Oscillation - Concepts And Studies. Surv Geophys 22: 321-381.

WANNER H ET AL. 2008. Mid- to Late Holocene climate change: an overview. Quat Sci Rev 27: 1791-1828.

WHITE JWC, BARLOW LK, FISHER D, GROOTES PM, JOUZEL J, JOHNSEN SIGFUS J, STUIVER M & CLAUSEN HB. 1997. The climate signal in the stable isotopes of snow from Summit, Greenland: Results of comparisons with modern climate observations. J Geophys Res C (12): Oceans 102: 26425-26440.

How to cite

EVANGELISTA H, DE SOUZA ECHER MP & ECHER E. 2022. Using wavelet decomposition method to retrieve the solar and the global air temperature signals from Greenland, Andes and East Antarctica $\delta^{18}O$ ice core records. An Acad Bras Cienc 94: e20210797. DOI 10.1590/0001-3765202220210797.

Manuscript received on June 1, 2021;
accepted for publication on August 4, 2021

HEITOR EVANGELISTA[1]
https://orcid.org/0000-0001-9832-1141

MARIZA P. DE SOUZA ECHER[2]
https://orcid.org/0000-0001-6706-8585

EZEQUIEL ECHER[2]
https://orcid.org/0000-0002-8351-6779

[1]Universidade do Estado do Rio de Janeiro, Laboratório de Radioecologia e Mudanças Globais/LARAMG/DBB/IBRAG, Pavilhão Haroldo L. Cunha, Subsolo, Rua São Francisco Xavier, 524, Maracanã, 20550-013 Rio de Janeiro, RJ, Brazil
[2]Instituto Nacional de Pesquisas Espaciais/INPE, Divisão de Heliofísica, Ciências Planetárias e Aeronomia, CEA II, Av. dos Astronautas, 1758, Caixa Postal 515, 12201-970 São José dos Campos, SP, Brazil

Correspondence to: **Ezequiel Echer**

E-mail: ezequiel.echer@inpe.br , ezequiel.echer@gmail.com

Author contributions

Heitor Evangelista da Silva: General concept of the manuscript/Paleoclimate description/ Paleoclimatic database compilation and text writing. Mariza Pereira de Souza Echer: Use of frequency decomposition methods, spectral analysis and text writing. Ezequiel Echer: General concept of the manuscript/ Long term and SSN description and text writing.